ELSEVIER

Coastal Engineering 41 (2000) 269–293

COASTAL ENGINEERING

www.elsevier.com/locate/coastaleng

Ocean forecasting in narrow shelf seas: application to the Spanish coasts

Juan Carlos Carretero Albiach*, Enrique Alvarez Fanjul, Marta Gómez Lahoz, Begoña Perez Gomez, Ignacio Rodríguez Sanchez-Arevalo

Programa de Clima Marítimo (Ente Público Puertos del Estado), Antonio López 81, Madrid E-28026, Spain

Abstract

The continental shelf surrounding the Spanish coast is very narrow. This is of great importance when studying the wave and surge dynamics in the region and contrasts with other well-studied regions like the North Sea, both in the physics and in the modelling techniques applied to obtain predictions of waves and sea surface elevation at the coastline. This paper describes those differences and presents the approach to the problem implemented in the wave and surge prediction system operational at Clima Marítimo (CM).

The narrowness of the Spanish continental shelf requires very high resolution grids to be applied to localised regions near the coast. The usual configuration of a local system nested to a global system (e.g. grids covering the North Sea nested to the European Centre for Medium Range Weather Forecasting global model) cannot be used in this case. Interpolation and coarse grid errors from boundary conditions provided by a global grid very near the coast will not be corrected by a small-scale local application. It was found that self-contained systems, solving in the same run the basin and local scales by means of variable grid spacing techniques, were the optimal solution. Some new techniques were developed in the process (two-way nesting for the wave generation model, a transfer function technique for the wave spectra) and implemented in the system. Although some of these developments have been already published [Gómez, M., Carretero, J.C., 1997. A two-way nesting procedure for the WAM model: application to the Spanish coast. J. Offshore Mech. Arctic Eng. 119 (February 1997).], the final set-up of both systems is presented here for the first time. Both systems are regularly verified with experimental data from the Spanish network of buoy and tide gauges. Results from this intercomparison are discussed in this paper.

* Corresponding author. Fax: +34-152-45-506.
E-mail address: juancc@puertos.es (J.C. Carretero Albiach).

PII: S0378-3839(00)00035-1

The PROMISE Spanish Coast Data Set was used to carry out much of the work presented here (i.e. the forcing and validation of the surge prediction system). This is a collection of physical oceanographic and meteorological data in the Bay of Biscay during stormy periods from November 1995 to March 1996.

Keywords: Operational oceanography; Surges; Waves; Spanish coast

1. Introduction

Along the Spanish coast, in the Atlantic Ocean (including the Canary Islands) and in the Mediterranean Sea (including the Balearic Islands), a common characteristic feature is found: the continental shelf is very narrow, ranging from 2 to 50 km wide (Fig. 1). This fact makes an important difference to the coastal dynamics compared with other well-studied regions such as the North Sea.

One of the tasks of Clima Marítimo (CM), a dependent group within the Spanish holding of harbours Puertos del Estado (PE), is to provide a wave and surge forecast to the Spanish harbours. The users of CM's operational forecast need predictions of sea conditions at the entrance of harbours, well inside the continental shelf, although out of the surf zone. During the development and implementation of these two systems, a number of problems had to be solved, in particular the challenge of numerical modelling of an open and exposed coast with a narrow continental shelf. In this paper, the approach to the problem for wave and sea level modelling, which eventually was implemented in CM's operational system, is described and discussed.

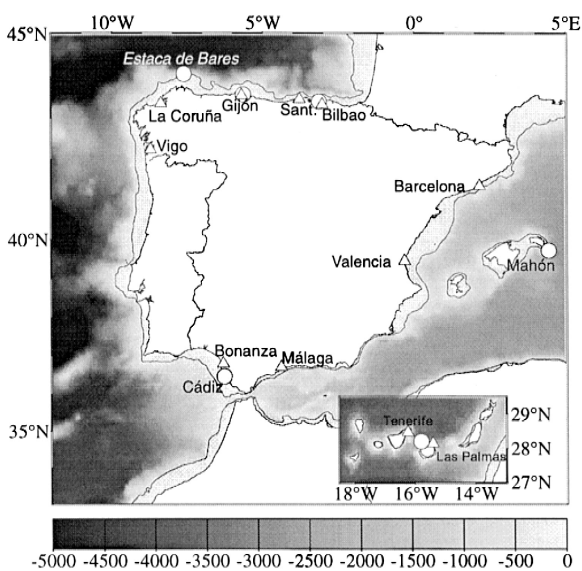

Fig. 1. Bathymetry in the Iberian Peninsula and Canary Islands region. The contour line corresponds to the 200 m isobath. Note also the position of the tide gauges (triangles) and the buoys (circles) used in this paper for model validation.

To carry out much of the work presented in this paper (i.e. the forcing and validation of the surge prediction system), the PROMISE Spanish Coast Data Set was used. This is a collection of physical oceanographic and meteorological data (wave parameters, wind speed and direction, atmospheric pressure, sea level residuals, etc.) in the Bay of Biscay during stormy periods between November 1995 and March 1996. The PROMISE Spanish Data set can be reached under the following Internet address: http://www.puertos.es/promise/ introduccionb1.html. Results derived from numerical simulations described in this paper were also incorporated as part of the mentioned data set.

This paper is structured as follows: first, theoretical introductions are provided for narrow shelf dynamics and modelling (Sections 2 and 3). Section 4 is devoted to wave dynamics for the Spanish coasts, and the solutions designed to provide forecasts in this region are described. The different approaches to solve the coastal region with higher resolution and reasonable computing cost are explained (one-point spectral propagation and model nesting). Extensive validation from buoy data is presented in every case. Section 2 is devoted to the surge dynamics and, as in the case of the waves, the methods employed to provide a forecast in the studied waters. Validation with data from the PROMISE Spanish Coast Data Set is also included. The main focus for both waves and surges is placed on the dynamics and basic ideas to provide forecasts rather than in the technical details of the operational systems. Finally, some conclusions are derived and ways forward are highlighted.

2. Narrow shelf surge and wave dynamics

The abovementioned narrowness of the shelf impacts on the surge and wave dynamics in the ways described below.

2.1. Waves

Wind waves generated in deep water far away from the coast propagate and reach the Spanish coast where they are modified by the bathymetry and coastline only in the last few kilometres (see the Cantabric Coast in the north of the Peninsula in Fig. 1). For this reason, the continental shelf plays a role only when predicting waves in coastal areas but not for navigation or offshore activities. A prediction system designed to forecast waves at the coast has to cope with the problem of solving, in the same run, the basin scale at which waves are generated, and the much smaller coastal scale where waves are modified. An additional peculiarity in this case is that the available buoy data usually come from nearshore moored buoys, which are not suitable for carrying out data assimilation as can be done with buoy data in other areas, e.g. the North Sea.

2.2. Sea level

The evolution of sea surface elevation during a storm surge event is strongly influenced by bathymetry. In seas with a wide continental shelf, such as the North Sea,

surge evolution is dominated by the wind. In those seas, extratropical surges can be very large (up to 4 m in the North Sea). At the Spanish coast, residuals are mostly produced by pressure variations. In fact, a first 'rough' estimate of the residuals in the Atlantic Spanish harbours can be obtained through the study of the time series of inverted atmospheric pressure records, although the effect of the wind can also be important during severe storms. The Mediterranean Sea is a special case, as the inverse barometer effect cannot be applied directly (Le Traon and Gauzelin, 1997). Garret (1983) developed a simple model of the Mediterranean, which includes two basins and two straits (Gibraltar and Sicily). This model, driven by the mean atmospheric pressures on the two Mediterranean basins, produces better results than a simple inverse barometric correction, and shows the importance of the Strait of Gibraltar in studying the barotropically induced sea surface elevation in the Mediterranean. Results from the numerical simulations presented here confirm this critical role. In narrow shelf seas, the limited effect of the wind over the shelf produces smaller surges (up to 1 m).

The barotropic set of equations contains nonlinear terms (see later description of the HAMSOM model equations). One of the effects of these terms is to transfer energy contained in one frequency to another (Bowden, 1983). For example, the M_2 tidal constituent generates harmonics (M_4, M_6) with frequencies that are multiples of the original. Also, the residual elevation during a storm surge is modified by nonlinear interactions with the tide. In very shallow seas, these nonlinear contributions cannot be neglected, becoming critical to predict the evolution of sea surface. In the North Sea and the English channel, for example, M_4 becomes an important harmonic and residuals cannot be properly predicted without the nonlinear contribution of energy from tides (Pugh, 1987). We will show that, for the Spanish coast, these nonlinear transfers are less important.

3. Narrow shelf surge and wave modelling

The modelling techniques and procedures needed to predict waves and surges at the Spanish coast are determined by the dynamical characteristics induced by the presence of a narrow shelf.

3.1. Waves

In seas with a wide coastal shelf, as is the case of the North Sea, shallow water applications of wave models are run at intermediate resolutions of around $1/4°$, covering scales of hundreds of kilometres, and a global model is used to provide boundary conditions to local models. Along the Spanish coasts, especially for the Atlantic coast, models able to predict waves at the coast need to be shallow water versions run on high resolution grids, less than $1'$. Beyond the shelf, there is no need for shallow model versions and high resolutions, except to avoid interpolation problems when boundary conditions to the local applications are provided.

Two approaches are possible in this case: (A) a number of local models run at high resolution implemented along the coast receiving boundary conditions from global

models or (B) a self-contained application covering all the generation area with some kind of variable grid spacing scheme, so as to gradually increase the resolution towards the coast, supplying the inputs to propagation models or transfer functions able to predict the waves at the coast.

The second approach (B) was chosen at CM for practical reasons (no boundary conditions had to be transferred or stored) and technical reasons (a gradual increase in the resolution towards the coast was deemed desirable to smooth the fields and to avoid interpolation errors). The system is described in detail in Section 4.

3.2. Sea level

In shelf seas, residuals are typically computed in the following way to take into account nonlinear interactions between tidal and meteorological forcing (Davies and Lawrence, 1994): first, a complete simulation, including tidal and atmospheric forcing, is performed; after that, a tidal simulation (with the major harmonic constituents, which contain most of the total tidal energy) is carried out for the storm simulation days. Residuals are obtained by subtracting sea surface elevations from both simulations. We will show that, in narrow shelf seas where nonlinear transfers are not so critical, similar results are obtained with the simpler method of computing residuals as the sea surface elevation derived from a simulation forced only by meteorological fields.

As previously mentioned, sea surface elevation at the Spanish coasts is determined mainly by atmospheric pressure, although during severe storms, the effect of the wind is also important. The typical width of the continental shelf at the Spanish coasts is 30 km and, therefore, the effect of the wind over these shallow regions cannot be solved in detail with the applied model resolution ($15' \times 10'$). There are two alternative ways to solve this problem (Vested et al., 1995). The first is to implement a set of nested models that allows a satisfactory solution for the shelf regions. The second option is to modify the depth of the near coast grid points in order to provide the model with a shallow region such that the effect of the wind can be taken properly into account. In this paper, we will explore this second and simpler option and we will show the benefits derived from its application.

4. Wave modelling for the Spanish coasts

The wave forecasting system operational at CM is based on two implementations of the WAM model (WAMDI Group, 1988; Komen et al., 1994), one for the Atlantic Ocean and one for the Mediterranean Sea. To obtain high resolution close to the Spanish coast without resorting to high resolution in the deep ocean, a two-way nesting scheme for the WAM model has been developed and implemented. The WAM grid then provides boundary conditions to applications of a high resolution wave generation model (WAVEWATCH) and a phase-averaged monochromatic wave propagation model (PROPS). For this last coupling of WAM and PROPS, a new approach has been developed. The coupling, which has an extremely low computation cost, is based on

linear theory and gives solutions only for those points of interest. This system is forced by wind fields supplied twice a day by Oceanweather Inc. (Cox et al., 1995).

4.1. Basin scale: the WAM model

The model run for this purpose is the standard WAM cycle 4 model (Günther et al., 1991), with some modifications carried out and implemented by CM in the model, although the physics in the standard cycle 4 version of the model remains untouched. The standard version of the model is well known and tested and is operational at several institutions (Carretero and Günther; 1992; Günther et al., 1992), so it will not be described here.

The grid spacing required to resolve the coast should be no more than 0.5°, but the computer costs prohibit consideration of such a high resolution for the whole area. One-way nesting was introduced as an option in cycle 4 of the model. The advantages of choosing a one-way nesting scheme to increase the resolution in an area as opposed to covering the whole basin with a fine grid are evident, but it was found that this nesting procedure is not applicable when the resolution has to be enhanced drastically, unless intermediate grids are placed between the coarse and the fine grid areas. This solution, in turn, requires excessive computing resources.

For our nested application to produce boundary conditions for coastal applications of a wave model, we need to enhance our resolution to a few kilometres. As already noted, the enhanced resolution in a nested scheme should be gradual, and this implies that many grids should be nested. In order to minimise the abovementioned problems, a two-way nesting approach was finally chosen. This scheme, given in Gómez and Carretero (1997), developed for CM's application of the model, works in practice as a variable grid spacing scheme in the sense that all grid points are integrated at the same time and that the grid spacing depends on the area being considered. The resolution is enhanced through consecutive rectangles of regular spacing. At the boundaries of these rectangles, the grid is not continuous, and some grid points obtain energy by interpolation and others by advection. Interpolation is still present for some grid points, but the resolution can be enhanced gradually, and this minimises the problems produced by linear interpolation. This method enables the user to enhance the resolution for more than one area in the same grid, and allows one to reach resolutions sufficiently high so as to produce boundary conditions for coastal applications (e.g. propagation models developed for harbours). To implement such a scheme in the model implies a new way of organising the grid, and a modification of the advection routine so as to make it compatible with the new grid arrangement. The problem is solved by covering the whole area with a grid as fine as the finest grid spacing defined by the user. Grid points are activated or deactivated to define different resolutions in different areas. Neighbouring points for energy advection are computed considering the resolution defined for the area — in practice, this means that non-active points are skipped in the advection. The propagation time step has to be reduced to satisfy the Courant–Friedrichs–Lewy (CFL) criterion, and to avoid reducing the source term integration time step as required in the standard version of the model, the code has been changed at CM so as to allow a propagation time step smaller than the source term integration time step.

Fig. 2 shows the advection scheme for a grid portion containing a border between rectangles of different resolution, filled circles indicate active grid points, and blank circles are deactivated points. It shows two types of grid points in the boundary, some getting energy by advection (A) and others by interpolation (I). For I-type grid points, the standard algorithm implemented in the model for spectra interpolation is carried out. For A-type grid points, the distance to the neighbours has to be taken into account when advecting energy. The grid spacings $\Delta\lambda$ (increment in latitude) and $\Delta\phi$ (increment in longitude) depend on the location of the grid point to be computed. Additionally, $\Delta\lambda$ and $\Delta\phi$ depend on which is the upstream neighbouring grid point, so these variables are also dependent on the direction θ of the spectrum component which is advected. The numerical implementation of the advection equation was modified to take into account these new dependencies, and an easy way for the user to define the grid was included in the user input files of the model.

4.2. WAM model implementation

Figs. 3 and 4 show the grid for the Atlantic and Mediterranean applications, and Table 1 the specifications of the WAM model for both grids.

4.3. Local scale: the WAVEWATCH model and the PROPS model

The ocean wind wave model, WAVEWATCH II (Tolman, 1991, 1992), a further improvement of WAVEWATCH developed by Dr. Hendrik L. Tolman, is a third-generation wave model which integrates a wave action conservation equation explicitly considering wave growth and decay, wave–wave interaction and dissipation due to white capping and wave–bottom interaction. Furthermore, it incorporates effects of unsteady and inhomogeneous currents on ocean waves. This model has been developed for high resolution applications in shallow waters considering interaction with ocean currents. The model has been modified at CM to make it capable of working as a nested application for a certain area, receiving boundary conditions from other spectral models.

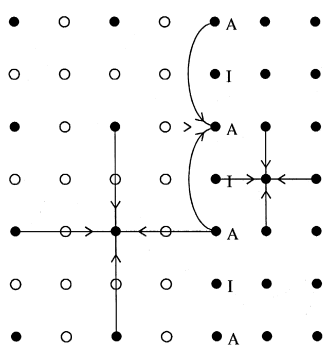

Fig. 2. Wave advection in the limit of areas with different resolution. A points get energy through advection and I points through interpolation.

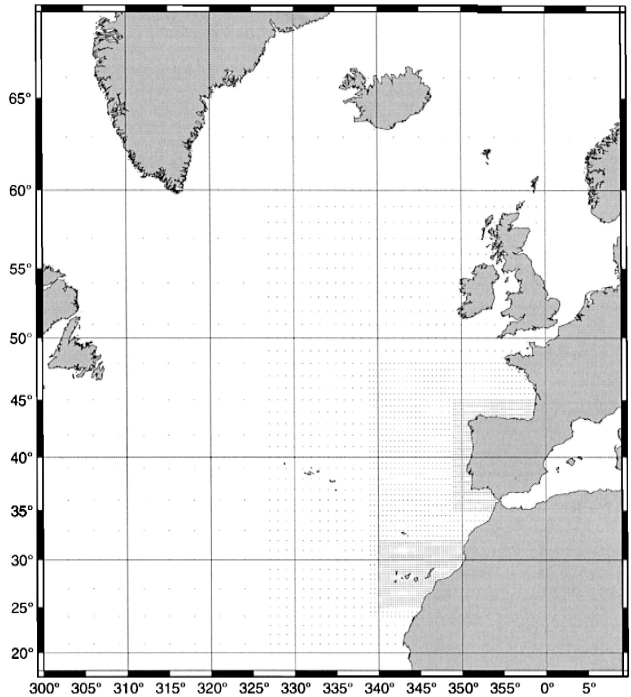

Fig. 3. WAM grid for the Atlantic Ocean.

Another modification to the code has been to introduce the possibility for the user to define a propagation time step smaller than the source term integration time step.

The PROPS model (Rivero and Arcilla, 1993; Garci, 1996), is a spectral wave propagation code able to propagate wave spectra into very shallow waters. The code solves the combined effects of shoaling, refraction, diffraction, wave–current interaction

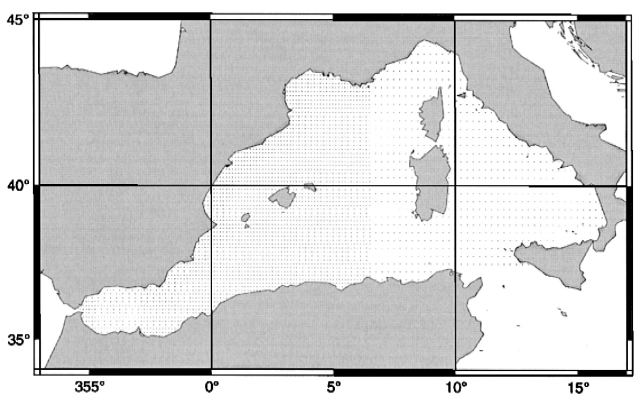

Fig. 4. WAM grid for the Mediterranean Sea.

Table 1
Model and grid specifications for the Spanish coast

Variable	Atlantic	Mediterranean
Model version	Deep water	Shallow water
Δt for propagation	600 s	300 s
Δt for source terms	1200 s	1200 s
Spectral directions	24	24
Spectral frequencies	25	25
Lowest frequency	0.041772 Hz	0.041772 Hz
Highest frequency	0.41145 Hz	0.41145 Hz
Northern limit	69°	45°
Southern limit	18°	34°
Western limit	60°	7°
Eastern limit	9°	17°
Coarsest grid spacing	3°	0.25°
Finest grid spacing	0.25°	0.125°

and energy dissipation due to wave breaking and bottom friction. In order to propagate a spectrum, the code follows this sequence: first, the wave spectra is discretised into a finite number of components (bins), then each component is propagated and, finally, the spectra is reconstructed. The model is a phase-averaged wave propagation code based on the wave action conservation equation, the irrotationality of the wave number, the dispersion relationship and, to take diffraction effects into account, the eikonal equation.

4.4. Local scale: WAVEWATCH and PROPS model implementation

Figs. 3 and 4 show that the WAM grids developed for the Atlantic Ocean and Mediterranean Sea are not connected through the Strait of Gibraltar. Waves generated in the Atlantic Ocean entering the Mediterranean Sea through the strait are not considered by the WAM model and this area has to be modelled with a resolution not smaller than 1 min to obtain reasonable results; this resolution allows roughly six grid points in the narrowest section of the Strait of Gibraltar. A local application of the WAVEWATCH model has been developed at CM covering the Gulf of Cadiz, Strait of Gibraltar and part of the Alboran Sea. This application is nested to the WAM grids for the Atlantic Ocean and the Mediterranean Sea. The boundary conditions are the WAM energy spectra modified as wave action spectra and interpolated in space and time. The coverage and grid points of the application are shown in Fig. 5, and Table 2 lists the main specifications.

A direct coupling between PROPS and WAM is not possible because of time constraints in an operational system. A new approach based on the idea of providing solutions only for those points of interest and not in the complete simulation domain has been developed. The new coupling system was developed with the assumptions that wave generation is negligible and linear theory can be applied. These assumptions are valid at most of the buoy positions and harbour mouths because the shelf is very narrow (small fetch) and the studied points are outside the surf zone. The effect of neglecting

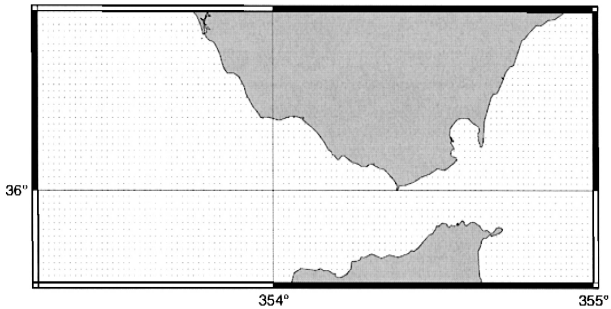

Fig. 5. WAVEWATCH grid for the Strait of Gibraltar.

bottom friction will be studied in more detail in the future, although propagation results presented in this paper show that is not critical for the purposes of coupling.

The coupling, to provide wave spectra in a selected point, is established as follows: once the simulation domain for the wave propagation model is given, PROPS is employed as a linear monochromatic model to propagate a set of regular wave trains corresponding to each component of the WAM spectra between the WAM point nearest to the coast (generally located in deep waters due to the narrow Spanish shelf) and the selected point. Simulations are performed for all the WAM frequencies and the directions corresponding to waves travelling to the coast. No breaking or bottom friction is herein considered.

The direction of propagation and the value of the coefficient K (the ratio between the propagated and incident wave height) resulting from the simulations are obtained at the selected point for each spectral component and in so-called 'wave transfer tables' The input variables of these tables are the angles and frequencies in which the WAM spectra are discretised and the outputs are the values of K and the direction of propagation

Table 2
WAVEWATCH model and grid specifications for the Strait of Gibraltar

Variable	Value
Model version	Shallow water
Δt for propagation	60 s
Δt for source terms	600 s
Spectral directions	24
Spectral frequencies	25
Lowest frequency	0.41772 Hz
Highest frequency	0.41145 Hz
Northern limit	36.75°
Southern limit	35.75°
Western limit	6.75°
Eastern limit	5°
Coarsest grid spacing	3°
Finest grid spacing	1′

Table 3
Characteristics of the buoys used in the verification

Location	Network	Type	Water depth (m)	Latitude N (°)	Longitude W (°)
Estaca de Bares	RAYO	Seatex	Deep water	44.065	7.62
Bilbao	REMRO	Waverider	50	43.4	3.14
Hijon	REMRO	Waverider	23	43.57	5.65
Las Palmas	RAYO	Seatex	Deep water	28.2	15.8
Mahon	EMOD	Wavescan	300	39.72	−4.44
Puerto de Cadiz	EMOD	Wavescan	65	36.46	6.30

angle at the selected point. Constructing these tables may be considered as a pre-processing operation.

The one-point spectral propagation code makes use of these tables to compute the propagated spectra. First, the energy density of each WAM spectrum component is multiplied by the square of the corresponding value of K (previously computed and stored in the wave transfer table). The use of the square of K is due to the fact that this coefficient describes the change in wave height, while the spectrum contains information on the energy density, proportional to the square of the wave height. The new value, computed by this method and corresponding to each component of the initial spectrum, is allocated to the new spectrum in components of the same frequency (linear theory) and directions obtained by the corresponding propagation angle. The propagated spectrum is computed by addition of the results of applying this process to all the components of the WAM spectrum. This allows the WAM spectra propagation to the coastal points of interest to be performed without a representative computational effort in addition to the prediction system.

Results obtained from this method are identical to those obtained with the linear version of the PROPS spectral model at the point of interest.

4.5. Wave simulation results

The outputs of the system, both predicted and analysed waves (waves produced with analysed winds), are regularly verified against measurements from the Spanish network of directional and scalar buoys. An example of the performance of the system is shown here. It corresponds to the skill of the analysed values of significant wave height (H_s) during the period May–October 1997, inclusive, when compared with buoy measure-

Table 4
Statistical results of the comparison of H_s between the WAM model output and buoy measurements

Ouptut	Sample	Mean buoy	Mean WAM	Correlation	Slope	Intercept	RMSE	Bias	Scatter
Estaca	496	1.712	1.568	0.855	0.72	0.33	0.416	−0.143	0.243
Palmas	445	1.393	1.231	0.751	0.72	0.23	0.319	−0.161	0.229
Mahon	1199	1.061	1.032	0.834	0.71	0.28	0.430	−0.029	0.405

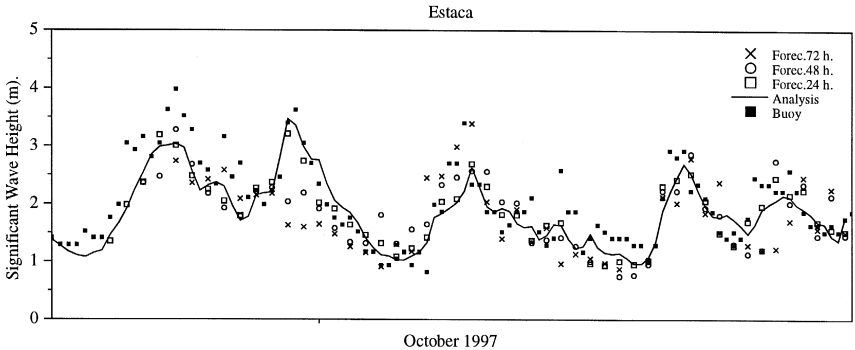

Fig. 6. Model and forecasted H_s values compared with the Estaca buoy measurements. The solid line corresponds to the analysed model values, squares to the +24 forecast, circles to the +48 forecast and crosses to the +72 forecast. Filled black squares are buoy measurements.

ments. The value of H_s for the model is derived in the usual way from the full bi-dimensional spectrum, and it is derived from the frequency spectrum for the buoy data (Eq. 1):

$$H_s = 4\sqrt{\int_f S(f)\,\mathrm{d}f}\,. \tag{1}$$

Table 3 shows the main features of the buoys which are used in this verification and Fig. 1 shows their location. For this verification, no time or space interpolation has been applied to the model output. The nearest model grid point for coincident output times has been compared with the buoy data.

The intercomparison, parameters are those commonly adopted for wave modelling. Three buoys have been used for this purpose: Estaca, Las Palmas and Mahon. These buoys are representative for three areas with different wave climate: the Cantabric Coast

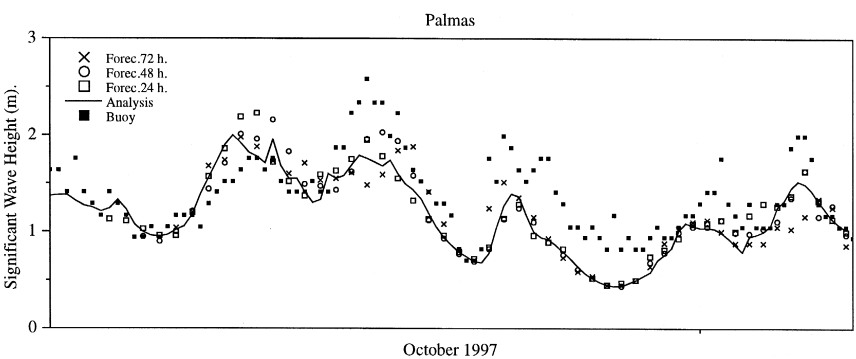

Fig. 7. Model and forecasted H_s values compared with the Palmas buoy measurements. The solid line corresponds to the analysed model values, squares to the +24 forecast, circles to the +48 forecast and crosses to the +72 forecast. Filled black squares are buoy measurements.

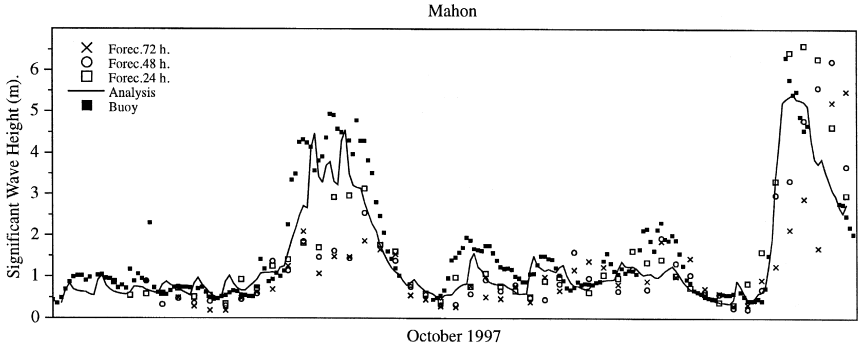

Fig. 8. Model and forecasted H_s values compared with the Mahon buoy measurements. The solid line corresponds to the analysed model values, squares to the +24 forecast, circles to the +48 forecast and crosses to the +72 forecast. Filled black squares are buoy measurements.

of Spain, subjected to waves produced by frontal depressions travelling form West to East; the Canary Islands, with waves frequently produced by trade winds; and the Mediterranean Sea, with highly variable winds which are very much determined by the orography of the mountains surrounding the basin. Although close to the coast, these buoys are in deep water and not sheltered by the coast, except for the Las Palmas buoy where directions sheltered by the islands cannot be accurately reproduced by the model at the present resolution.

Table 4 shows the skill of the WAM model output for the analysed period when compared with buoy measurements and Figs. 6–8 show time series of H_s for the month of October compared with the buoy measurements. Analysed and forecast values produced by the model are plotted along with buoy measurements.

Analysed values from the model follow the measurements quite well except for Las Palmas where a more accurate definition of the coastline of the islands is needed to better reproduce the directions sheltered by other islands. A tendency to underestimate peaks can be observed — this causes the slopes of the regression fitting to be less than unity. Wind fields every 3 h would probably lead to a more accurate reproduction of the peaks. It can be seen that because the period considered includes the summer months, the mean values for both model and buoy outputs are low, as there were very few storms. Unfortunately, this means that the representativeness of the derived statistics is reduced.

The verification of the WAVEWATCH output in this example has been carried out against the measurements of a buoy moored at the Harbour of Cadiz. This buoy

Table 5
Statistical results of the comparison of H_s between the WAVEWATCH model output and Cadiz buoy measurements

Output	Sample	Mean buoy	Mean WAM	Correlation	Slope	Intercept	RMSE	Bias	Scatter
Analysis	684	0.759	0.849	0.733	0.87	0.19	0.309	0.090	0.407

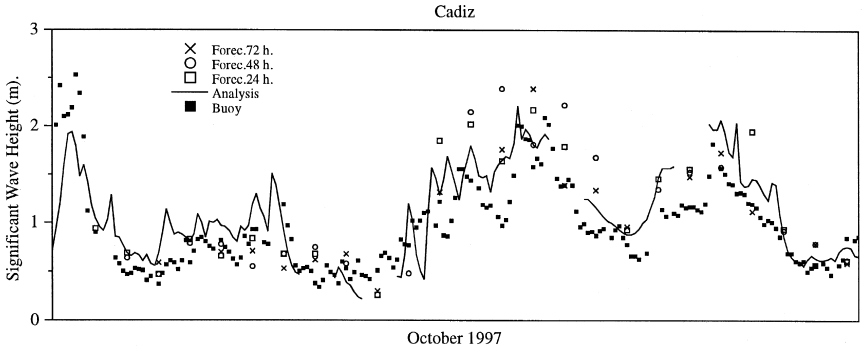

Fig. 9. Model and forecasted H_s values compared with the Cadiz buoy measurements. The solid line corresponds to the analysed model values, squares to the +24 forecast, circles to the +48 forecast and crosses to the +72 forecast. Filled black squares correspond to buoy measurements.

measures waves subject to refraction and attenuation by shoaling in front of the harbour. The small mean values of H_s, with long periods of time when wave heights are below 1 m, produce statistical results for the verification that are not really representative of the skill of the analysed waves produced by the model (Table 5). However, inspection of Fig. 9 shows a very good reproduction of the H_s peaks — something that has been observed since the implementation of the model. Although in this example intention is not to show verifications of the peak period, it has to be mentioned that the prediction of this parameter for the harbour is extremely good, something much more relevant in this case than wave height due to resonance problems in the harbour.

The one-point spectral propagation coupling between WAM and PROPS is carried out to improve the WAM output by taking into account coastal effects not resolved by the WAM model. Of course, the skill of the forecast will not be better than that of the WAM model, which supplies the input to the PROPS model. Results from the coup-

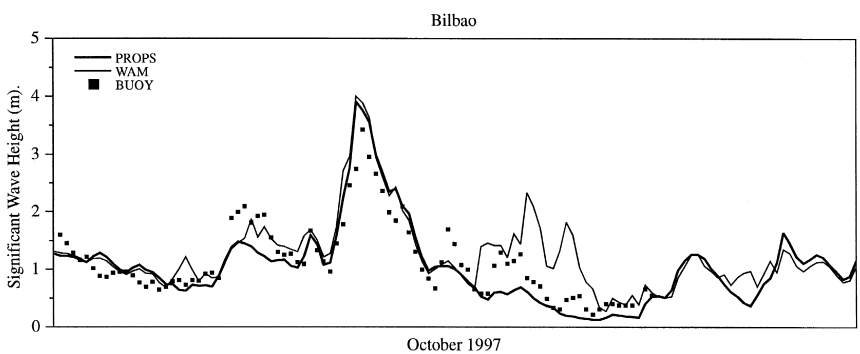

Fig. 10. Analysed WAM and WAM–PROPS values of H_s compared with Bilbao buoy measurements. Thick line corresponds to the WAM output, fine line to the WAM–PROPS output and filled black squares to buoy measurements.

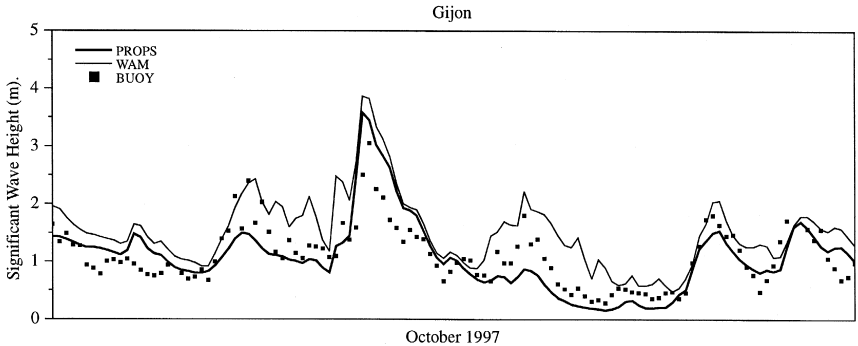

Fig. 11. Analysed WAM and WAM–PROPS values of H_s compared with Gijon buoy measurements. Thick line corresponds to the WAM output, fine line to the WAM–PROPS output and filled black squares to buoy measurements.

ling can be seen in Figs. 10 and 11. The clear improvement in the 'bias' (see Tables 6 and 7), especially for Gijon, shows clearly the need for this coupling if waves at the mouth of the harbour are to be predicted. Statistical analysis of other time periods (not presented in this paper) shows that the coupled system provides the best results during storm events when an accurate prediction is really needed.

5. Tide and surge modelling at the Spanish coast

This section is devoted to the study of the tides and surges at the Spanish coast by means of numerical modelling and through the analysis of the data contained in the PROMISE Spanish Coast Data Set. The model runs correspond to the whole PROMISE data set period (November 1995–March 1996). This period was extremely stormy on the Spanish coasts and, therefore, is quite appropriate for testing a surge model. Values from the above data set are used to validate the meteorological input and to compare the results of the model with the sea level residuals obtained by means of the REDMAR tide gauge network (Pérez and Rodriguez, 1994) managed by PE. Results from the simulations also form part of the mentioned data set.

The main objective is to analyse the behaviour of our surge prediction system (named Nivmar), employing the period corresponding to the PROMISE data set (November 1995–March 1996) as a benchmark case. The atmospheric forcing employed in these

Table 6
Statistical results of the comparison of H_s between the WAM analysis and WAM–PROPS analysis and the Bilbao buoy

Output	Sample	Mean buoy	Mean WAM	Correlation	Slope	Intercept	RMSE	Bias	Scatter
WAM	388	1.047	1.131	0.819	0.90	0.19	0.358	0.084	0.343
PROPS	388	1.047	1.043	0.880	0.98	0.02	0.289	−0.003	0.276

Table 7
Statistical results of the comparison of H_s between the WAM analysis and WAM–PROPS analysis and the Gijon buoy

Output	Sample	Mean buoy	Mean WAM	Correlation	Slope	Intercept	RMSE	Bias	Scatter
WAM	400	0.979	1.340	0.870	1.04	0.32	0.465	0.361	0.475
PROPS	400	0.979	1.032	0.839	0.92	0.13	0.304	0.053	0.310

test simulations (six hourly fields of winds at 10 m and pressures) was obtained from the same source (fields supplied by the Spanish Met. Office, Instituto Nacional de Meteorología, and produced by their operational system based on the HIRLAM model) as the data operationally employed to force Nivmar. The model domain of the HIRLAM model (resolution $0.5° \times 0.5°$) covers the entire HAMSOM model domain and the data are bilinearly interpolated to the HAMSOM grid.

The computation of residuals was performed by means of the procedure explained in Section 1 that takes into account the nonlinear transfers between astronomical and meteorological forcings. An independent simulation, forced only by atmospheric fields, is employed to compute a second data set of residuals which does not include the nonlinear influence of tides. Comparison of both sets of residuals will show the small statistical importance of the mentioned transfers at this region, scale and resolution.

5.1. The HAMSOM model

The HAMSOM model (Backhaus, 1983, 1985; Rodriguez and Alvarez, 1991; Rodriguez et al., 1991; Stronach et al., 1993; Alvarez Fanjul et al., 1997), developed by the Institut für Meereskunde and by CM, is a three-dimensional multi-level (z-coordinate) finite difference model (Arakawa C grid) based on the barotropic set of Reynolds equations:

$$\frac{\partial \boldsymbol{u}}{\partial t} + \boldsymbol{u}\frac{\partial \boldsymbol{u}}{\partial x} + \boldsymbol{v}\frac{\partial \boldsymbol{u}}{\partial y} + w\frac{\partial \boldsymbol{u}}{\partial z} + \frac{1}{\rho}\frac{\partial P}{\partial x} = f\boldsymbol{v} + A_{\mathrm{h}}\left[\frac{\partial^2 \boldsymbol{u}}{\partial x^2} + \frac{\partial^2 \boldsymbol{u}}{\partial y^2}\right] + \frac{\partial \tau_x}{\partial z}, \tag{2}$$

$$\frac{\partial \boldsymbol{v}}{\partial t} + \boldsymbol{u}\frac{\partial \boldsymbol{v}}{\partial x} + \boldsymbol{v}\frac{\partial \boldsymbol{v}}{\partial y} + w\frac{\partial \boldsymbol{v}}{\partial z} + \frac{1}{\rho}\frac{\partial P}{\partial y} = -f\boldsymbol{u} + A_{\mathrm{h}}\left[\frac{\partial^2 \boldsymbol{v}}{\partial x^2} + \frac{\partial^2 \boldsymbol{v}}{\partial y^2}\right] + \frac{\partial \tau_y}{\partial z}, \tag{3}$$

where $\boldsymbol{u}$ and $\boldsymbol{v}$ are the vector velocity components; t the time; P the pressure; ρ the water density; f the Coriolis frequency; τ_x and τ_y are the components of the stress vector; and A_{h} the horizontal eddy viscosity. The formulation is completed with the continuity and hydrostatic equations:

$$\frac{\partial \boldsymbol{u}}{\partial x} + \frac{\partial \boldsymbol{v}}{\partial y} + \frac{\partial w}{\partial z} = 0, \tag{4}$$

$$\frac{\partial P}{\partial z} = -\rho g, \tag{5}$$

where g is the gravitational acceleration.

HAMSOM is written in Cartesian coordinates. To account for the convergence of meridians, all distances in the horizontal axis are computed as a function of latitude and the cell volume so considered is distorted for mass conservation purposes.

The code uses a two-time-level numerical scheme (present and future). Some equation terms are treated semi-implicitly (like pressure gradient and vertical diffusive stress) and the remaining ones explicitly (momentum advection, horizontal diffusion). The Coriolis term is treated following the approach developed by Wais (1985).

Bottom stress is parameterised by a quadratic law in terms of current velocity:

$$\vec{\tau}_b = C_b \vec{u}_L |\vec{u}_b|, \tag{6}$$

where $\vec{u}_b$ stands for the horizontal vector velocity at the bottom level of the model and $\vec{u}_L$ is the vertically averaged horizontal velocity in a friction layer close to the bottom. C_b is the dimensionless drag coefficient. A 'classical' value of 0.0025 was selected for all the runs. Bottom friction is treated in a semi-implicit way, $\vec{u}_b$ being computed in the future time and $\vec{u}_L$ in the present. An additional sophistication is introduced when computing this last transport: it is calculated in a layer with a constant thickness (30 m), independently of the vertical discretisation present at the grid point. This helps to avoid large jumps in the values of friction in areas where the bottom level of the model is very thin (Rodriguez and Alvarez, 1991).

Wind stress is computed from wind fields using the Charnock parameterisation (Charnock, 1955), which can be tuned by means of the so-called Charnock constant (α).

Although not employed in this paper, a baroclinic version of the code is also available.

5.2. Model implementation

The model domain covers an area extending from 20°N to 48°N in latitude and from 34°W to 30°E in longitude. The bathymetry employed in the simulations (Fig. 12), based on the DTM5 data set (GETECH, 1995), was built by using a variable grid size scheme in order to reduce the number of computational points and, consequently, the computation time. This scheme is based on a zooming technique. A region spanning from 25°N to 16.48°N and from 20°W to 30°E keeps a constant resolution of $10' \times 15'$. The grid size in the rest of the domain is increased progressively towards the boundaries, the size of each cell being incremented by a factor of roughly 1.1 with respect to its inner neighbour. Small deviations are present in this factor in order to place the boundaries on a nonfractional latitude (20°N) and longitude (34°W).

In the north coast of the Iberian Peninsula, the available bathymetry did not correctly represent the existing narrow shelf. As a consequence, the effect of the wind was initially underestimated in the simulations. In order to improve the model results, the depths of the grid points near the coast were modified in this region. After some tuning, it was found that changing the depth of the two rows (or columns) of grid points adjacent to the land to 10 and 50 m produces optimal results. These changes in the bathymetry greatly improve the results of the model in the region.

The time step employed in both the benchmark presented in this paper and in the Nivmar system is 10 min, and A_h is kept constant at 200 $m^2\ s^{-1}$. After some tuning

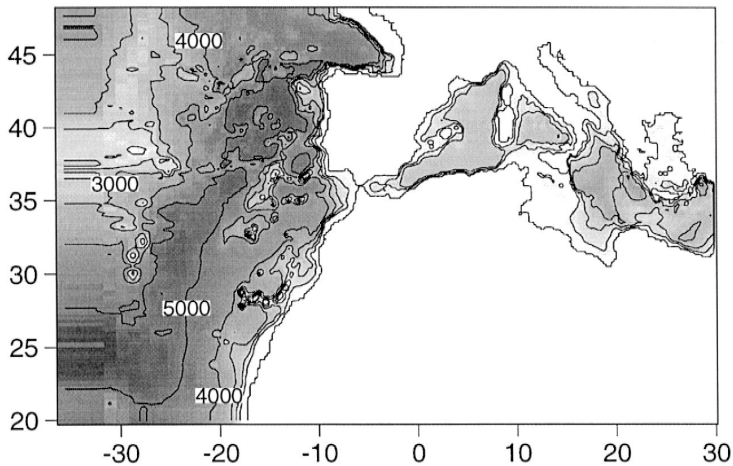

Fig. 12. Bathymetry employed in the storm surge simulations. Resolution in the west part of the domain is poor due to the variable grid size scheme employed and to the fact that the first two model columns are equal in order to implement a zero gradient boundary condition for the transports.

(Alvarez Fanjul et al., 1997), it was found to be convenient to use a high value for the Charnock constant ($\alpha = 0.032$). Presently, the model used is vertically integrated within Nivmar.

Tidal forcing was introduced by imposing the harmonically predicted elevation at the open boundaries. A routine (Akima, 1978) was used to interpolate amplitude and phase values from the FES95.2 data set to the boundary points of the higher resolution HAMSOM grid.

Direct astronomical forcing is neglected. Some authors handle the self-attraction and loading of the ocean tide by a simple scalar multiplier of the elevations in the momentum equations (e.g. Accad and Pekeris, 1978). This is only a crude approximation, and it is particularly poor in near-coastal areas (Francis and Mazzega, 1990). We have therefore chosen to ignore this relatively small forcing term.

When simulating storm surges, the elevation at the Atlantic open boundaries was corrected by means of the inverse barometer effect.

5.3. Tide simulations results

In order to study the behaviour of the model when solving tidal dynamics, seven different runs were performed to simulate the M_2, S_2, N_2 and K_2 semidiurnal and O_1, K_1 and P_1 diurnal harmonics one by one. Results (not shown) were compared with those from previous runs (Alvarez Fanjul et al., 1997) derived from older data sets (ETOPO 5, NGDC, 1988; for bathymetry and Ray et al., 1994 for tidal constants at the open boundaries). The comparison shows a considerable improvement in the solutions, especially at the French coast, where model errors were larger. For example, the M_2 amplitude at Port Tudy derived from the simulation based on FES95.2 and DTM5

(152.7 cm) is much closer to the real value (148.3 cm) than the amplitude obtained when employing the other data sets (174.0 cm).

5.4. Storm surge simulations results: comparison with the PROMISE Spanish Coast Data Set

Fig. 13 shows a comparison of the residuals obtained by numerical simulation with those measured by the REDMAR during the PROMISE Spanish Coast Data Set Period (see Fig. 1 for locations of the tide gauges). The three stations in Fig. 13 are representative of different regions of the Spanish Coast (Canary Islands, Mediterranean coast and Iberian Peninsula Atlantic coast). In order to establish a comparison, the frequency of the simulated data was changed from 10 min (time step of the model) to 1 h (period between two measurements). The mean value of the simulated series was

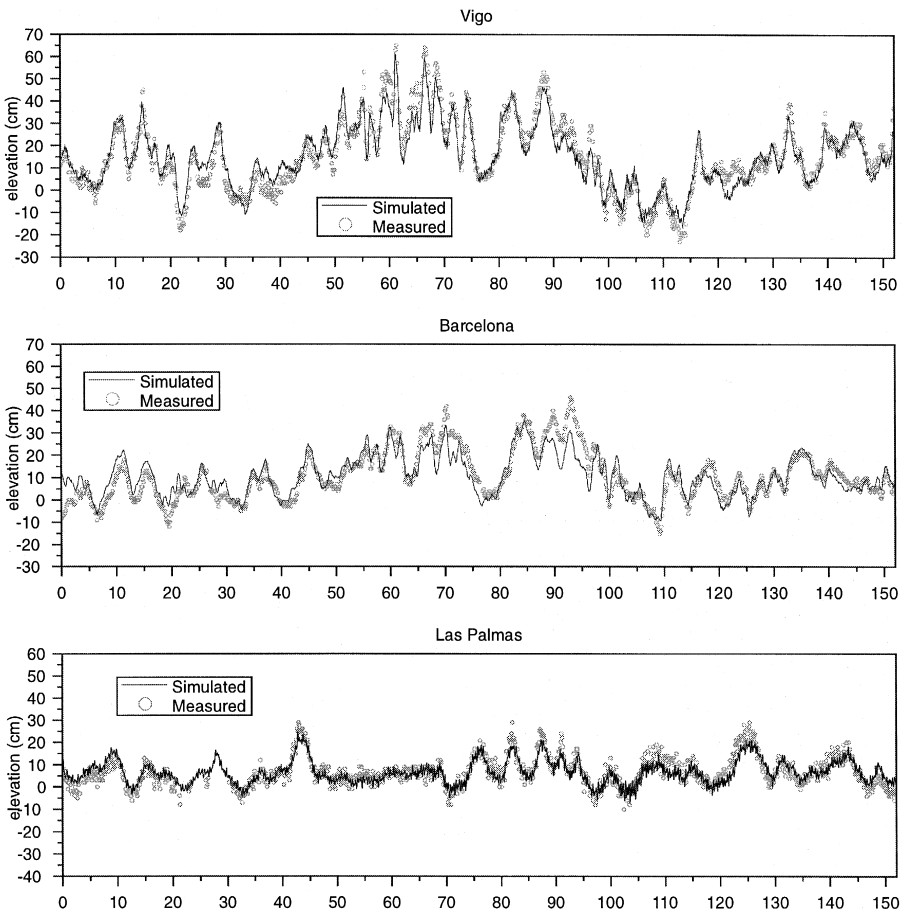

Fig. 13. Measured and simulated residual at three stations: Vigo in the Atlantic coast, Barcelona in the Mediterranean coast and Las Palmas at the Canary Islands.

modified to the value of that measured. These techniques are usually employed in hindcast studies of surge simulations (Vested et al., 1995).

Table 8 shows a statistical comparison between simulated and measured series at the stations in Fig. 1.

Model results at the Cantabric and Galician coast (stations from Bilbao to Vigo) are quite satisfactory, especially considering that this is a very stormy period. Maximum errors are around 20 cm, typical values for root mean square error (RMSE) are 5 cm, and the correlation index is very high (0.95 for Vigo). Most of the largest peaks are correctly reproduced, including extreme storms (i.e. 66 cm at La Coruña on January 6 (day 67) of the simulated period).

The residuals measured at Bonanza show larger differences (maximum error RMAX = 69 cm) from the simulated data. This gauge station is located at the mouth of the Guadalquivir River, and residuals are strongly influenced by the river outflow. Since this variable is not included in the simulations, the observed discrepancies are to be expected. In periods where no significant outflow from the river was present, the agreement between measurements and simulations improves considerably.

For the Mediterranean Sea, RMSE and RMAX have the same orders of magnitude as for the Atlantic coast, having lower vales of correlation index CI (minimum of 0.85 for Valencia). These lower values of CI may be due to two different reasons. The first one is the quality of the winds. At the resolution of the atmosphere model ($0.5° \times 0.5°$), wind solutions are better at the Atlantic coast than in the Mediterranean coast (the eastward travelling atmospheric structures are affected by the complex topography of the Iberian Peninsula and, therefore, atmospheric fields are more complex to solve at the east side of the Peninsula; Garcia-Moya, personal communication). Future use of atmospheric fields of higher resolution ($0.2° \times 0.2°$) will mean an improvement in the sea elevation solutions in this region. The second cause of discrepancies could be the low resolution of the ocean model in the region of the Strait of Gibraltar (one grid point at the trait).

Table 8
Statistical comparison of measured and simulated residuals

Station	Nr	$\bar{X}$	RMSE	RMAX	m	b	CI
Bilbao	3648	7.89	5.66	21.03	0.82	1.44	0.90
Santander	3571	9.30	5.72	24.73	0.88	1.14	0.91
Gijón	3382	−0.68	6.03	19.70	0.88	−0.08	0.89
La Coruña	3648	17.58	5.89	20.69	0.81	3.30	0.92
Vigo	3614	15.23	5.04	20.86	0.81	2.82	0.95
Bonanza	3483	11.59	10.17	66.93	0.44	6.54	0.80
Málaga	3648	11.63	5.14	26.12	0.69	3.66	0.86
Valencia	3612	11.84	5.75	17.38	0.63	4.42	0.85
Barcelona	3630	10.88	5.14	20.04	0.71	3.15	0.89
Tenerife	3610	9.20	4.24	17.08	0.64	3.35	0.77
Las Palmas	3392	6.73	3.70	11.60	0.65	2.34	0.83

Nr is the number of records, $\bar{X}$ is the mean value of the measured residuals (mean value of simulated residual is corrected to this value), RMSE is the root mean square error, RMAX is the maximum error, m and b are the slope and the interception of the linear fit, respectively, and CI is the correlation index.

The role of this region in the evolution of sea surface elevation in the Mediterranean Sea can be seen in Fig. 14. This figure shows the results at Barcelona (compared again with measured residuals) of a similar simulation, but with the strait closed (the grid point corresponding to the strait was artificially converted to land). From the analysis of the figure, it is clear that, if the Mediterranean Sea is isolated from the Atlantic, the response of the model becomes worse. The statistical analysis confirms this: the correlation index decreases from 0.89 to 0.62, the RMSE increases from 5.15 to 8.72 cm and the slope of the linear fit reduces from 0.71 to 0.37. These results are coherent with the ideas behind the simple analytic model developed by Garret (1983) (Candela et al., 1989; Le Traon and Gauzelin, 1997), where sub-inertial flows through the strait and barotropically induced sea surface elevation in the two main Mediterranean basins are basically determined by the relations between the mean atmospheric pressures over the two basins and over the Atlantic. Consequently, it is clear that a higher resolution representation of the Strait region could imply an even better solution at the Mediterranean Spanish coast.

The agreement at the Canary Islands is highly satisfactory, with RMSE values as low as 3 or 4 cm.

In spite of the narrowness of the shelf, the effect of the wind on the sea surface elevation during severe storms cannot be neglected. Fig. 15 shows a comparison of different predictions of residuals with the measurements at La Coruña during a very stormy period. The residual measured on January 6 (66 cm) is the largest one ever recorded by the REDMAR at this station. The atmospheric situation corresponds to a deep low (954 mb) located at the west of Ireland and a cold front crossing over La Coruña at 0600 h. Associated with these atmospheric structures, strong winds were present parallel to the coast. The prediction, computed by means of the inverse barometer correction, strongly underestimates the surge height. Therefore, it is necessary to include the wind effect over the narrow shelf to solve the surge characteristics. The other two lines show the behaviour of the model with and without the previously explained changes to the depth of the grid points adjacent to the coast. The bathymetry corrections improve the solutions, mainly on the peaks of days 6 and 11. It is important to note that, in the largest surge recorded at La Coruña, the error of the model with the bathymetry corrected is only around 5 cm. The surge on day 8 is not correctly reproduced even with the modifications because the atmospheric model underestimated the wind parallel to the coast (figure not shown).

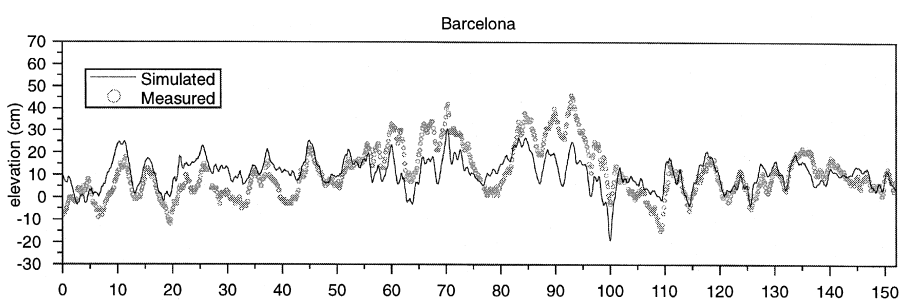

Fig. 14. Measured and simulated residual at Barcelona. Simulation performed with the Strait of Gibraltar closed. Compare with Fig. 13.

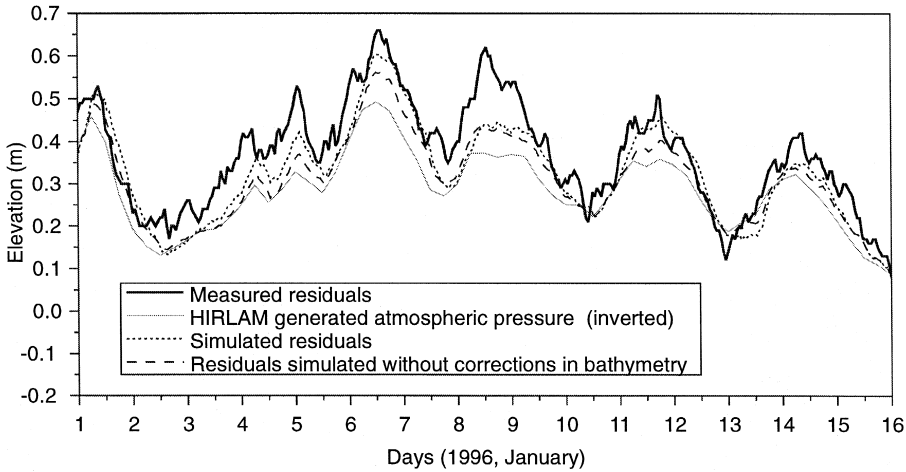

Fig. 15. Comparison of measured and simulated residuals at La Coruña. Solid thin line corresponds to the elevation predicted by means of the Inverse Barometer Correction method.

In order to estimate the importance of the nonlinear transfers between meteorological and astronomical forcing, a second set of residuals was generated by simply forcing the model with the meteorological fields (without taking tidal forcing into account). We found that the differences between both sets of residuals are very small, being maximum during large storms (largest difference of 2.5 cm at Bilbao). These differences do not represent a significant statistical improvement (RMSE at Bilbao with nonlinear transfer was 5.66 and without this contribution was 5.65). Smaller differences in the results imply that in this region, barotropic dynamics is basically linear. This agrees well with the observed small amplitude shallow water harmonics. Therefore, at this scale and resolution, residuals can be predicted in narrow shelf seas without taking into account the nonlinear transfers of tidal energy (the tidal elevation can be added later in the post-processing stage). This procedure is simpler than the one needed in shelf seas (like the North Sea) involving two simulations. It is also important to note that, when studying semi-enclosed regions near the coast (such as bays), the nonlinear transfers could be of higher relative importance when determining sea elevation, but this hypothesis cannot be studied at the resolution employed in this paper.

6. Conclusions

When compared with shelf seas like the well studied North Sea, coastal dynamics surrounding the Spanish coast is strongly influenced by the presence of a narrow continental shelf.

For the sea surface elevation, the effect of the wind on the residuals is much smaller and, therefore, surges are less important. Nonlinear effects between tides and surges are not critical for computing surge elevations. Waves approach the coast from open waters and only in the last few hundreds of meters are they modified by the continental shelf.

These differences in the dynamics are reflected in the ways numerical prediction is performed at CM compared to other centres such as those surrounding the North Sea. When designing the forecast systems, the fact that the entire basin and the coastal platform had to be modelled in the system posed a number of problems. A key point was to increase the resolution to resolve the coastal platform. Several techniques are applied in CM's systems and results are shown in this paper (these include variable grid spacing and two-way nesting, spectral point propagation, artificial modifications of the bathymetry). An extensive validation of both wave and surge systems is also included in the paper. The results show the importance of the straits of Gibraltar when computing sea surface elevation in the Mediterranean Sea.

Future research in modelling for operational purposes (where operational models mean those codes which are run as the core of prediction systems) has always to keep in mind the balance of the benefits produced by new developments and the computing costs (in terms of time, storage space, etc.) that these innovations introduce to the system. For this reason, non-operational versions of models are usually one step ahead of those run daily in operational systems. The implementation of new versions as operational versions is more a technical or numerical problem than a scientific problem. In summary, the main question is how to improve predictions at a reasonable cost.

To improve the system described in this paper, extra effort is needed in the development of numerical schemes to increase the resolution near the coast or to produce a baroclinic ocean forecast at low computational cost. At the same time, the input to the system has to be improved. In coastal ocean forecasting, one of the main sources of errors is the predicted atmospheric data near the coast. To provide, in real time, unsheltered experimental data for assimilation is crucial, and this is especially true for the Mediterranean Sea where wind patterns are mostly conditioned by the surrounding orography. Atmospheric data provided by coastal buoys would be extremely useful for this purpose.

Acknowledgements

PROMISE (Pre-Operational Modelling in the Seas of Europe) was a MAST III programme funded by the European Commission, MAS3-CT9500025.

References

Accad, Y., Pekeris, C.L., 1978. Solution of the tidal equations for the M_2 and S_2 tides in the world oceans from a knowledge of the tidal potential alone. Philos. Trans. R. Soc. London, Ser. A 290, 235–266.

Akima, H., 1978. A method of bivariate interpolation and smooth surface fitting for irregularly distributed data points. ACM Trans. Math. Software 4 (2), 148–159.

Alvarez Fanjul, E., Pérez Gómez, B., Rodríguez Sánchez Arévalo, I., 1997. A description of the tides in the Eastern North Atlantic. Prog. Oceanogr. 40, 217–244.

Backhaus, J.O., 1983. A semi-implicit scheme for the shallow water equations for application to shelf sea modelling. Cont. Shelf Res. 2 (4), 243–254.

Backhaus, J.O., 1985. A three-dimensional model for simulation of shelf sea dynamics. Dtsch. Hydrogr. Z. 38 (4), 164–187.

Bowden, K.F., 1983. Physical Oceanography of Coastal Waters. Ellis Horwood, London.
Candela, J., Winant, C.D., Briden, H., 1989. Meteorological forced sub-inertial flows through the straits of Gibraltar. J. Geophys. Res. 94, 12667–12679.
Carretero, J.C., Günther, H., 1992. Wave forecast performed with the WAM model at the ECMWF. Statistical analysis of a one-month period (November 1988). ECMWF Technical Report No. 68, UK.
Charnock, H., 1955. Wind stress on a water surface. Q. J. R. Meteorol. Soc. 81, 639–640.
Cox, A.T., Greenwood, J.A., Cardone, V.J., Swail, V.R., 1995. An interactive objective kinematic analysis system. Fourth International Workshop on Wave Hindcasting and Forecasting, October 16–20, 1995, Banff, Alberta, Canada.
Davies, A.M., Lawrence, J., 1994. Examining the influence of wind and wave turbulence on tidal currents, using a three-dimensional hydrodynamic model including wave–current interaction. J. Phys. Oceanogr. 24, 2441–2460.
Francis, O., Mazzega, P., 1990. Global charts of ocean tide loading effects. J. Geophys. Res. 95 (C7), 11411–11424.
Garret, C., 1983. Variable sea level and strait flows in the Mediterranean: a theoretical study of the response to meteorological forcing. Oceanol. Acta 6, 79–87.
GETECH, 1995. Geophysical Exploration Technology Internal Report. Department of Earth Sciences. University of Leeds, UK.
Garci, E., 1996. A spectral wave propagation model. MSc Thesis, UPC, Barcelona, Spain, 117 pp.
Gómez, M., Carretero, J.C., 1997. A two-way nesting procedure for the WAM model: application to the Spanish coast. J. Offshore Mech. Arctic Eng. 119, February.
Günther, H., Hasselman, S., Janssen, P.A.E.M., 1991. WAM model cycle 4. Technical Report No. 4, Deutsches Klima Rechen Zentrum, Germany.
Günther, H., Lionello, P., Janssen, P.A.E.M., Bertotti, L., Brüning, C., Carretero, J.C., Cavaleri, L., Guillaume, A., Hansen, B., Hasselman, S., Hasselman, K., de las Heras, M., Hollingsworth, A., Holt, M., Lefevre, J.M., Portz, R., 1992. Implementation of a third-generation ocean wave model at the European Centre for Medium-Range Weather Forecasts. ECMWF Technical Report No. 68, UK.
Komen, G.J., Cavaleri, L., Donelan, M., Hasselmann, K., Janssen, P.A.E.M., 1994. Dynamics and Modelling of Ocean Waves. Cambridge Univ. Press, UK.
Le Traon, P.-Y., Gauzelin, P., 1997. Response of the Mediterranean mean sea level to atmospheric pressure forcing. J. Geophys. Res. 102 (C1), 973–984.
NGDC, 1988. Data Announcement 88-MGG-02. Digital Relief of the Surface of the Earth. NOAA, National Geophysical Data Center, Boulder, CO.
Perez, B., Rodriguez, I., 1994. REDMAR. Spanish harbours tidal gauges network. Processing of tidal data. Publicación No. 57 de Clima Marítimo.
Pugh, D.T., 1987. Tides, Surges and Mean Sea Level: A Handbook for Engineers and Scientists. Wiley, London, 472 pp.
Ray, R.D., Sanchez, B.V., Cartwright, D.E., 1994. Some extensions to the response method of tidal analysis applied to TOPEX/POSEIDON. EOS, Trans. Am. Geophys. Union 75, 108, Abstract, Spring Meeting Supplement.
Rivero, F.J., Arcilla, A.S., 1993. Propagation of linear gravity waves over slowly varying depth and currents. Proceedings on ''WAVES '93'' Symposium, New Orleans, USA. pp. 518–532.
Rodriguez, I., Alvarez, E., 1991. Modelo Tridimensional de Corrientes. Condiciones de aplicación a las costas españolas y análisis de resultados para el caso de un esquema de mallas anidadas. Publicación no. 42 del Programa de Clima Marítimo.
Rodriguez, I., Alvarez, E., Krohn, J., Backhaus, J., 1991. A mid-scale tidal analysis of waters around the northwestern corner of the Iberian Peninsula. Computer Modelling in Ocean Engineering '91, Balkema.
Stronach, J.A., Backhaus, J.O., Murty, T.S., 1993. An update on the numerical simulation of oceanographic processes in the waters between Vancouver Island and the mainland: 24. The GF8 model. Oceanogr. Mar. Biol. Annu. Rev. 31, 1–86.
Tolman, H.L., 1991. A third-generation model for wind waves on slowly varying, unsteady and inhomogeneous depths and currents. J. Phys. Oceanogr. 21, 782–797.
Tolman, H.L., 1992. Effects of numerics on the physics in a third-generation wind wave model. J. Phys. Oceanogr. 22, 1095–1111.

Vested, H.J., Nielsen, J.W., Jensen, H.R., Kristensen, K.B., 1995. Skill assessment of an operational Hydrodynamic Forecast system for the North Sea and Danish Belts. Quantitative skill assessment for coastal ocean models. AGU 373–398.

Wais, R., 1985. On the relation of linear stability and the representation of Coriolis terms in the numerical solution of the shallow water equation. Doctoral Thesis. Hamburg University.

WAMDI Group, Hasselmann, S., Hasselman, K., Janssen, P.A.E.M., Komen, G.J., Bertotti, L., Lionello, P., Guillaume, A., Cardone, V.C., Greenwood, J.A., Reistad, M., Zambresky, L., Ewing, J.A., 1988. The WAM model – a third-generation ocean wave prediction model. J. Phys. Oceanogr. 18, 1775–1810.